

DTIC FILE COPY

AD A102620

EEV

12

AD

TECHNICAL REPORT ARBRL-TR-02336

LASER-EXCITED OPTO-ACOUSTIC
PULSES IN A FLAME

William R. Anderson
John E. Allen, Jr.
David R. Crosley



June 1981



US ARMY ARMAMENT RESEARCH AND DEVELOPMENT COMMAND
BALLISTIC RESEARCH LABORATORY
ABERDEEN PROVING GROUND, MARYLAND

Approved for public release; distribution unlimited.

818 10 030

Destroy this report when it is no longer needed.
Do not return it to the originator.

Secondary distribution of this report by originating
or sponsoring activity is prohibited.

Additional copies of this report may be obtained
from the National Technical Information Service,
U.S. Department of Commerce, Springfield, Virginia
22161.

The findings in this report are not to be construed as
an official Department of the Army position, unless
so designated by other authorized documents.

*The use of trade names or manufacturers' names in this report
does not constitute endorsement of any commercial product.*

UNCLASSIFIED

SECURITY CLASSIFICATION OF THIS PAGE (When Data Entered)

REPORT DOCUMENTATION PAGE		READ INSTRUCTIONS BEFORE COMPLETING FORM
1. REPORT NUMBER TECHNICAL REPORT ARBRL-TR-02336	2. GCVT ACCESSION NO. <i>AD-A102 620</i>	3. RECIPIENT'S CATALOG NUMBER
4. TITLE (and Subtitle) LASER-EXCITED OPTO-ACOUSTIC PULSES IN A FLAME -	5. TYPE OF REPORT & PERIOD COVERED BRL Technical Report	
7. AUTHOR(s) William R./Anderson John E./Allen, Jr.* David R./Crosley**	6. PERFORMING ORG. REPORT NUMBER	
9. PERFORMING ORGANIZATION NAME AND ADDRESS US Army Armament Research and Development Command US Army Ballistic Research Laboratory ATTN: DRDAR-BL Aberdeen Proving Ground, MD 21005	8. CONTRACT OR GRANT NUMBER(s)	
11. CONTROLLING OFFICE NAME AND ADDRESS US Army Armament Research and Development Command US Army Ballistic Research Laboratory ATTN: DRDAR-BL Aberdeen Proving Ground, MD 21005	10. PROGRAM ELEMENT, PROJECT, TASK AREA & WORK UNIT NUMBERS <i>1L161102AH43</i>	
14. MONITORING AGENCY NAME & ADDRESS (if different from Controlling Office)	12. REPORT DATE <i>JUNE 1981</i>	
	13. NUMBER OF PAGES <i>42</i>	
16. DISTRIBUTION STATEMENT (of this Report)	14. SECURITY CLASS. (of this report) <i>UNCLASSIFIED</i>	
	15a. DECLASSIFICATION/DOWNGRADING SCHEDULE	
17. DISTRIBUTION STATEMENT (of the abstract entered in Block 20, if different from Report)		
18. SUPPLEMENTARY NOTES *NAS-NRS Resident Research Associate; present address: Goddard Space Flight Center, Greenbelt, MD 20770 **Present address: Molecular Physics Lab, SRI International, Menlo Park, CA 94025		
19. KEY WORDS (Continue on reverse side if necessary and identify by block number) Optoacoustic effect Combustion Fluorescence Alkali atoms Quenching		
20. ABSTRACT (Continue on reverse side if necessary and identify by block number) (clt-jmk)		
<p>Pulsed pressure waves are produced by energy transfer from electronically excited Na or Li atoms seeded in an acetylene-air flame; the excitation is provided by a resonantly tuned, pulsed laser. Temperature increases of approximately one degree within the flame produce signals easily detected by a microphone. A description of the phenomenon is given, and preliminary results are presented for two possible applications: localized speed-of-sound measurements and quenching rate determinations.</p>		

TABLE OF CONTENTS

	Page
LIST OF ILLUSTRATIONS.	5
I. INTRODUCTION	7
A. Laser Probes and Combustion Chemistry.	7
B. Opto-acoustic pulses	8
II. EXPERIMENTAL DETAILS	9
A. Apparatus.	9
B. Qualitative Observations	15
C. Magnitude of the Pressure Wave	15
D. Form of the Pressure Wave.	16
III. APPLICATIONS AS A PROBE.	19
A. Concentration Measurements	19
B. Temperature Measurements: Speed of Sound.	23
IV. QUENCH RATE MEASUREMENTS	26
V. 4P LEVEL PUMPING	29
VI. CONCLUSIONS.	34
REFERENCES	37
DISTRIBUTION LIST.	39

Accession For	Serial
YRS	BY
RECD BY	PERIODIC
SEARCHED	TYPE
INDEXED	SEARCHED
SERIALIZED	INDEXED
FILED	FILED
Justification	
By _____	
Distribution/	
Availability Codes	
Avail and/or	
Special	

P

LIST OF ILLUSTRATIONS

Figure	Page
1. Experimental arrangement. The laser scanner, and a spectrometer often used for fluorescence observations, are not shown.	10
2. Oscilloscope trace of an opto-acoustic pulse. The time scale is 20 μ sec/cm, and the trace is triggered as the laser fires. Data such as those shown in Figure 2 are obtained from the difference between first two extrema, using the dual channel boxcar. The later oscillations with smaller amplitude are quite reproducible from pulse to pulse for fixed geometry and stable flame conditions	11
3. Opto-acoustic pulse signal as a function of laser frequency.	15
4. Output of the monitoring photodiode as the laser (with 6 cm ⁻¹ bandwidth) is scanned through the region of the D-lines. Zero corresponds to no laser intensity, so there is about fifteen percent absorption here.	14
5. Dependence of pressure wave amplitude on flame-to-microphone distance r	17
6. Oscilloscope traces of opto-acoustic signal waveform, for 4 different geometrical arrangements. Each results from a single laser pulse. Horizontal axis: 20 μ sec per major division	18
7. Microphone signal as a function of beam diameter (related to the optical saturation studies) showing that microphones of three different diameters yield the same relative response .	20
8. Dependence of the microphone signal on laser power, at power densities much lower than saturation values.	21
9. Dependence of the microphone signal on NaI concentration; presumably the Na concentration in the flame follows the solute concentration	22
10. Schematic illustration of the measurement of the speed of sound. On three different laser pulses, the laser beam is fired into the flame at three different positions, and the arrival time of the pressure pulse at the microphone is measured	24

LIST OF ILLUSTRATIONS (Cont'd)

Figure	Page
11. Schematic illustration of a system near optical saturation. Two level models are illustrated in (1) and (2); it is these which are pertinent to the treatment in the text. The multilevel model (3) requires the incorporation of relaxation rate parameters.	27
12. Plot of M^{-1} vs. I^{-1} , in the form of Eq. (4), for low laser power (large beam diameter).	30
13. Plot of M^{-1} vs. I^{-1} , in the form of Eq. (4), for high laser power (focussed beam).	51
14. Inverse of the pressure-wave amplitude versus inverse of the spectral-power density. Error bars represent estimates of the readability of the boxcar output. The line is an unweighted least-squares fit	52

I. INTRODUCTION

A. Laser Probes and Combustion Chemistry

The application of lasers to the study of combustion processes offers a wealth of information of diverse kinds. Many of these new techniques - in particular laser-excited fluorescence, ordinary Raman scattering, and coherent anti-stokes Raman spectroscopy - are aimed at the measurement of concentrations of individual molecular species at partial pressures ranging from several atmospheres down to 10⁻¹⁰ torr.¹ The use of scanning lasers permits one to map out energy level population distributions within ground electronic states, with an ease and accuracy previously possible only for excited states. From such information can be obtained temperatures corresponding to different degrees of freedom. Measurement of laser absorption line-shapes within flames provides data on energy transfer rates and translational temperatures. The recent successful observation of two-photon excitation of Na in a 1-atm pressure flame² suggests numerous possibilities for probing those species now inaccessible by present-day commercially available lasers with one-photon excitation.

The use of the full arsenal of these laser techniques so far demonstrated would provide a nearly complete experimental characterization of a process undergoing combustion. Of course, the use of lasers means, almost necessarily, a high degree of spatial resolution: focusing to 100 μ beam diameter is generally easy. Pulsed lasers of various types yield concomitant temporal resolution down to several nsec. Consequently spatial profiles, over time periods unblurred by turbulence, can be obtained for these quantities of interest. It should be noted that, in addition, laser probes are non-perturbative. That is, they introduce no physical barriers into the gas flow or provide surfaces which could cause heterogeneous catalysis influencing the chemistry. Although the presence of particulate matter can be a serious problem, extremes of temperature and pressure offer no hostility to the laser beam itself.

The field likely to benefit most from this detailed picture is that of combustion chemistry. The information on transient, reactive species will provide the key to the mechanistic chemical kinetics heretofore usually only inferred from the composition of final products.

¹A. C. Eckbreth, P. A. Bonczyk and J. F. Verdieck, "Review of Laser Raman and Fluorescence Techniques for Practical Combustion Diagnostics", United Technologies Research Center Report R77- 52665-6, Hartford, CT, February 1977.

²J. E. Allen, Jr., W. R. Anderson, D. R. Crosley and T. D. Fansler, "Energy Transfer and Quenching Rates of Laser-Pumped Electronically Excited Alkalies in Flames", Seventeenth Symposium (International) on Combustion, Leeds, England, August 1978.

Data on state distributions will directly address the questions of disequilibrium in combustion systems, widely recognized as existing but seldom accounted for in mechanistic schemes. In fact, this combination of experimental probes using laser-based techniques together with theoretical chemical kinetic modelling on modern large computers has been heralded³ as promising - finally - significant advancement in the enormously complex problem of the chemistry of combustion. An understanding of the chemistry pertinent to ballistic systems will undoubtedly require such models tied in detail to copious laser-based experiments (as well as measurements with other techniques) under controlled laboratory conditions and proven by agreement with the necessarily more limited data available on real systems.

Nearly all of the currently available laser probe methods rely on the scattering or emission of light as the mode of detection. While this can be a highly sensitive method under many conditions, there are other situations in which it is less suitable. For example, high excited state quenching rates reduce the degree of emitted fluorescence, and Raman-scattered photons could be absorbed by some interfering molecular species. One recent alternative method is the optogalvanic effect,⁴ in which the yield of collisionally produced ions is enhanced by promotion, using laser excitation, to excited electronic states lying nearer to the ionization continuum than does the ground state.

B. Opto-acoustic pulses

We describe here the observation and characterization of another means of detecting the occurrence of selective absorption of tuned laser radiation. This is the production of a pulsed opto-acoustic effect -- pulsed sound waves -- within a flame operating at atmospheric pressure, following deposition of the laser energy into an electronic transition.

The flame is seeded with alkali atoms and a pulsed laser is tuned to the appropriate absorption line. While some of the electronically excited atoms fluoresce, the vast majority lose their energy by collision with other gases present in the flame. This energy ultimately (though rapidly) is converted into translational kinetic energy of the flame gases, producing a pulsed pressure wave which expands from the region illuminated by the laser. Quantitative measurements are made using a microphone, and show that the technique is very sensitive and accurate, and perturbs neither the gas dynamics nor chemical kinetics of the flame. Because the phenomenon itself depends on the rapid

³D. Hartley, M. Levy and D. Hardesty, "Physics in Combustion Research", *Physics Today*, December 1975, 36-47.

⁴R. B. Green, R. A. Keller, P. K. Schenck, J. C. Travis and C. G. Luther, "Opto-Galvanic Detection of Species in Flames", *J. Amer. Chem. Soc.* 98, 8517-8518 (1976).

collisional conversion of electronic to translational energy (through the intermediary of molecular vibration), the signal is thus not reduced at high pressure as is the fluorescence. The results have provided directly useful information as well as projections concerning the sensitivity of the technique.

The opto-acoustic effect in general, *viz.*, the conversion of optical to acoustical energy through absorption and collisional quenching, has long been known as a means of sensitively detecting the absorption of radiation.⁵ What is newly demonstrated here is the nature of its occurrence following pulsed excitation, and the existence of the effect under *in situ* conditions on a 1-atm pressure flame burner (in contrast to the typical mode of operation using specially constructed cells at low pressure).

In addition to exploiting its detection capabilities, we have also utilized the effect to perform measurements of the speed of sound within the flame on a spatially resolved basis. These data provide information on the translational temperature of the flame gases. This aspect may prove especially useful for environments too hostile to admit thermocouple probes or processes too rapid to obtain usable thermocouple response.

The actual mode of formation of the pressure wave -- the fluid dynamics aspect -- is not investigated in any detail in these experiments. Observations have been made of the form of the pressure wave produced; it appears to be dictated by density gradients in the flame and surrounding atmosphere. Some modification of the experiment might permit the waveform to be used to extract bulk energy transfer rates, but we have not pursued that end.

Most of the experiments to be described were carried out pumping the 3P state of Na. We have been unable to detect opto-acoustic pulse formation when pumping the 4P level, and we conclude that the net effective conversion of electronic to translational energy, at least over the salient time scale, is less efficient for this level. In conjunction with this experiment, we also consider some of the results on energy transfer pathways among excited states of Na in the flame, obtained using multiphoton excitation of fluorescence.²

II. EXPERIMENTAL DETAILS

A. Apparatus

The experimental arrangement is depicted in Figure 1. The flame is a fuel rich mixture (1.5 times stoichiometric) of C₂H₂ and air, and the slot burner is a standard type used for atomic absorption analysis. Na is

⁵R. Y. Pao (ed.), *Optoacoustic Spectroscopy and Detection*, Academic Press, New York, 1977.

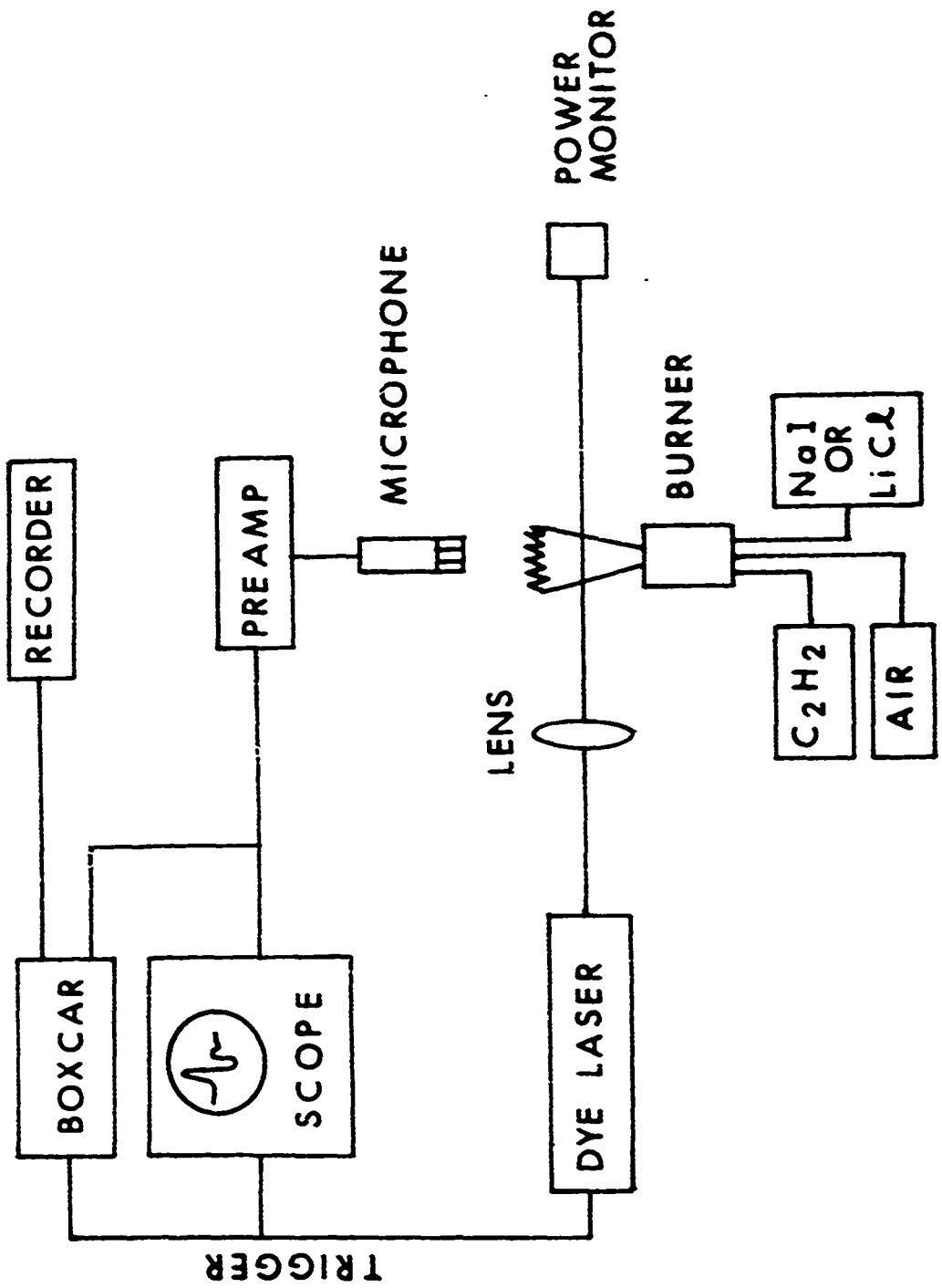


Figure 1. Experimental arrangement. The laser scanner, and a spectrometer often used for fluorescence observations, are not shown.

introduced by aspiration of NaI solution; many of the experiments were carried out at a Na concentration of the order of 10^{10} atoms cm^{-3} , as determined from both absorption and absolute fluorescence measurements. Additionally, a few experiments have been run using Li as the seed atom, or with Na in a CH_4 /air flame. The experiments are carried out at heights ranging from 0.5 to 3 cm above the surface, that is, in the region of the secondary reaction zone containing partially combusted gases.

The laser used is a Chromatix CMA-4, a commercially available flash-lamp pumped tunable dye laser having a pulse duration of 1 μsec . Although the laser is capable of delivering 10 mJ/pulse in the region of the Na resonance lines, it was here operated typically at < 1 mJ/pulse. The bandwidth is nominally 3 cm^{-1} and can be narrowed to 0.16 cm^{-1} by insertion of an etalon. (In a separate experiment, not further described here, opto-acoustic pulses have also been observed with a N_2 -laser-pumped-dye laser. The 5 nsec pulse lengths available with this instrument offer useful versatility with the techniques).

The laser is focused to a few mm beam diameter and directed into the flame at a spot ~ 2 cm above the burner surface. When the laser is tuned to either of the two components of the $3^2\text{P}-3^2\text{S}$ transition in Na, the energy released in the quenching of the resonantly excited 3P state produces a pressure wave which propagates outward from the region illuminated by the laser. This sound wave is detected by a condenser microphone located ~ 4 cm from the flame. After amplification, the microphone signal is fed to an oscilloscope and to a boxcar (gated) integrator, both of which are triggered by a pulse from a photodiode detecting the laser pulse itself. Figure 2 shows an oscilloscope photograph of a single pressure wave.

In Figure 3 is exhibited a recorder tracing of the amplitude of the pressure wave signal vs. laser frequency. The laser is operated here in its narrowed mode and automatically scanned over the wavelength region which includes both doublet components. The spikes marked 'etalon reset' are artifacts of the scanning sequence. It is clear that the pressure waves result from the resonant electronic excitation and not from some other mode of laser energy deposition within the flame gases, such as laser-induced breakdown of the flame gases.

The laser power was usually monitored by a laser calorimeter behind the flame. An alternate method involved splitting off a small portion of the beam before its entry into the flame and directing it to a spectrometer outfitted with a photomultiplier. These detectors also served at times for measurement of absorption and fluorescence. In addition, the optogalvanic signal, also in the form of pulses, was occasionally monitored. All four phenomena - absorption, fluorescence, optogalvanic pulses, and optoacoustic pulses - occur simultaneously when the laser is tuned to a resonance. Figure 4, shows a measurement of the laser power incident upon the photodiode as the laser is scanned across the D-lines at large (6 cm^{-1}) bandwidth. (This run was made at very high

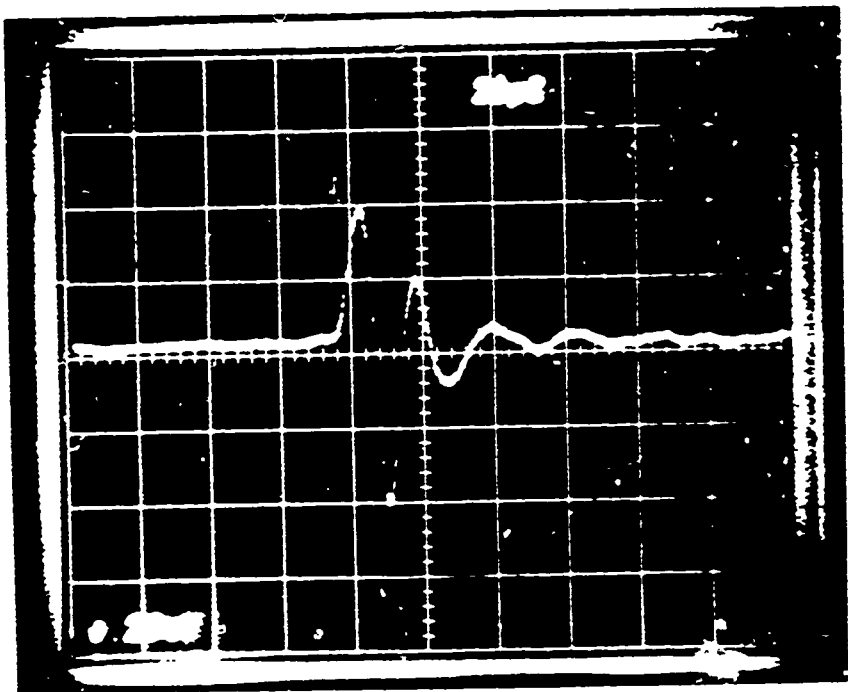


Figure 2. Oscilloscope trace of an optic-acoustic pulse. The time scale is 20 μ sec/cm, and the trace is triggered as the laser fires. Data such as those shown in Figure 2 are obtained from the difference between first two extrema, using the dual channel boxcar. The later oscillations with smaller amplitude are quite reproducible from pulse to pulse for fixed geometry and stable flame conditions.

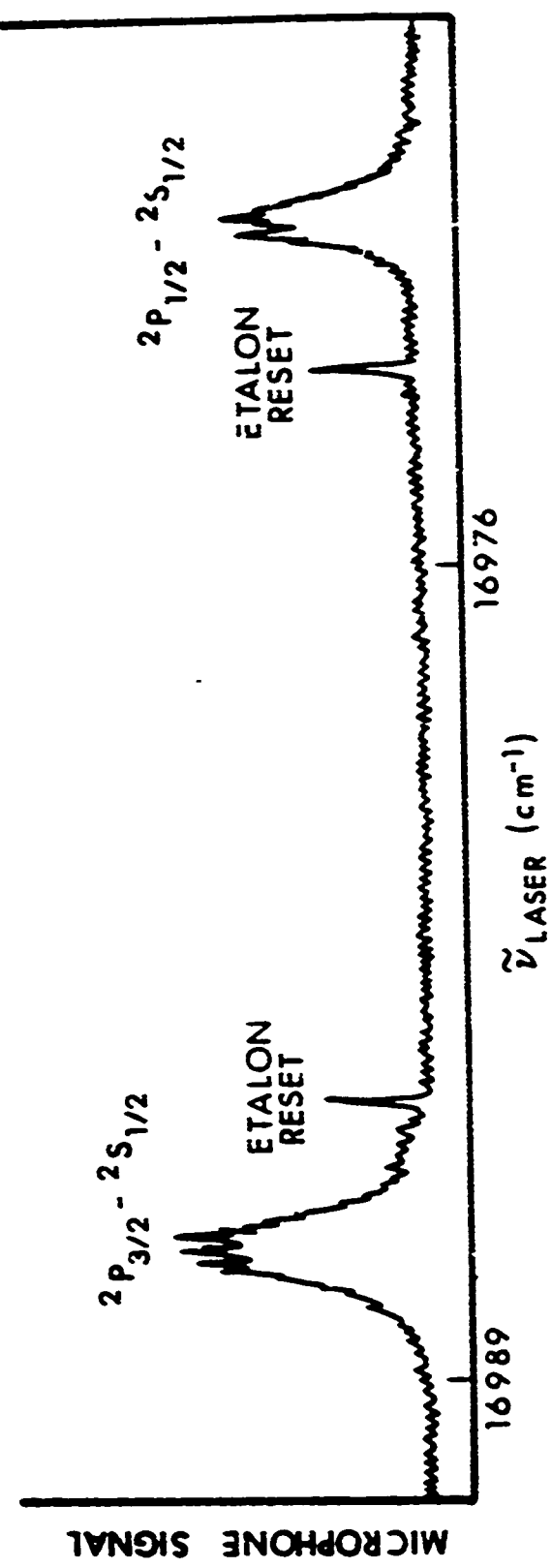


Figure 3. Opto-acoustic pulse signal as a function of laser frequency.

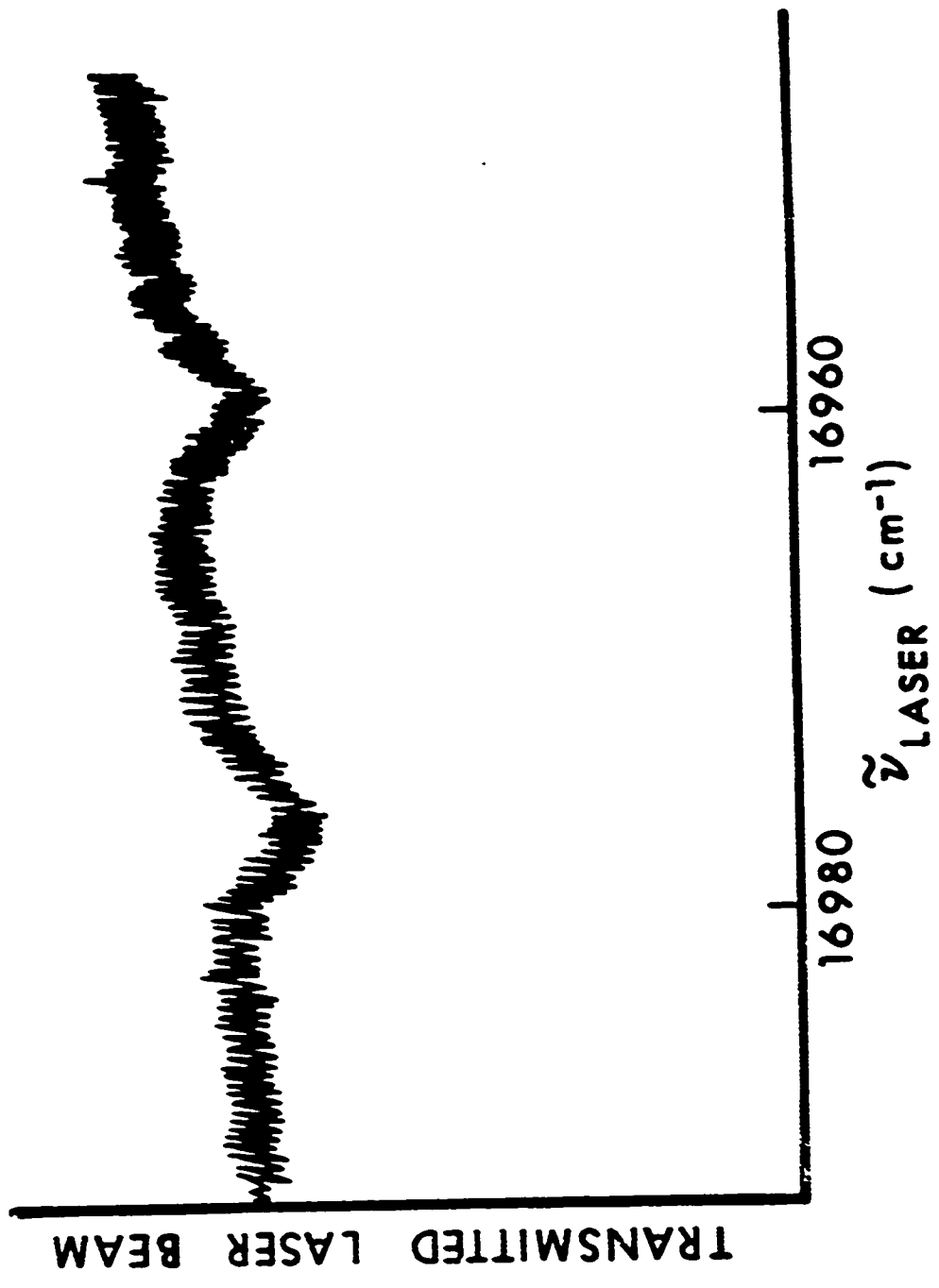


Figure 4. Output of the monitoring photodiode as the laser (with 6 cm^{-1} bandwidth) is scanned through the region of the D-lines. Zero corresponds to no laser intensity, so there is about fifteen percent absorption here.

Na density). From these runs, we can measure the amount of laser energy absorbed.

Not shown in Figure 1 is a spectrometer, with associated optics and photomultiplier, which was used to measure the fluorescence from the Na - particularly in those experiments² involving ultraviolet and two-photon excitation.

B. Qualitative Observations

When the laser is tuned to one of the resonance lines, the pulsed pressure wave is produced. At relatively high sodium density, so that a hundred microjoules or more of laser energy are absorbed, this wave is readily audible to an observer located within a few meters of the burner. In fact, the normal procedure for coarse manual tuning of the laser is to locate the resonance lines by listening for the sound wave.

As measured by the microphone and displayed on the oscilloscope the waveform shows a sharp rise as the sound wave reaches the detector, followed by a series of oscillations typically diminishing in magnitude. (See Figure 2). The two boxcar gates were set to correspond to the first minimum and first maximum of the waveform; the difference between these values was output to the recorder and constitutes the 'microphone signal' used below to denote the magnitude of the pressure wave.

C. Magnitude of the Pressure Wave

From the information directly available from the experiment, we can only speculate on the mode of formation of the pressure wave. Collisional quenching of the excited state transfers the Na electronic energy into vibrational levels of the flame gases (as demonstrated by an experiment on electronic-to-vibrational-to-electronic energy transfer between Na and Li in the same flame²). This energy is then rapidly converted to translational energy, resulting in translational heating of the region illuminated by the laser beam. Because sound travels only about 1 mm during the 1 usec heating time, and the laser beam is typically a little larger than this, we envision the energy deposition as resulting in a slightly hotter region where the laser beam has passed through the flame. A small shock wave may be initially formed; if so, it soon degrades into a pressure wave, and propagates outward through the flame.

We describe a particular, though typical, experiment to measure the absolute laser energy deposited and the resulting pressure wave amplitude. The Na absorbs 0.22 mJ from a single laser pulse, as the beam traverses a 1 cm path through the flame, with a diameter of 15 mm. Over 99% of the excited atoms are quenched by collisions under our conditions, so this is the amount of energy transferred into translation.

The flame gases are assumed diatomic here, with a density appropriate to 1 atm and the flame temperature (from speed of sound measurements

described below) of 2300°K . The irradiated volume of 1.75 cm^3 thus has a heat capacity of 0.54 mJ/degree and is heated 0.64°K . This is a truly negligible perturbation compared with the temperature of the flame gases themselves. A pressure rise of 0.22 torr within the heated volume is calculated using the ideal gas law.

At the microphone, the amplitude of the resulting pressure wave will be lower, because of the outward expansion of the wave. In these experiments, it is the pressure amplitude (not energy density) which is measured. A fall-off inversely proportional to the distance τ between flame and microphone is thus expected. Figure 5 shows a plot of the microphone response vs. τ^{-1} , verifying this dependence.

We can then calculate the amplitude anticipated at the microphone. For the geometry used here, an amplitude of 0.044 torr would result at the microphone. The measured value, using a calibrated microphone, is 0.15 torr. In view of concerns about the homogeneity of the laser beam over its spatial profile, some uncertainties in the measurement of the path length, and especially the lack of knowledge concerning the actual mode of formation of the pressure wave, we consider this to be reasonable agreement, confirming our simple physical picture.

D. Form of the Pressure Wave

The waveform of the sound wave is quite complex and we have examined it extensively, although no quantitative information could be extracted. As noted above, it is quite reproducible from pulse to pulse for a fixed geometry of laser/flame/microphone. If, however, this geometry is changed, considerable differences result. Figure 6 shows four oscilloscope traces for four different geometrical arrangements. The scope is triggered on the left by the photodiode, and the time scale here is $20 \mu\text{sec/cm}$. (The amplitude referred to throughout this paper is measured by setting the two boxcar gates to sample the first positive and negative extrema of the waveforms, and taking the difference.) The characteristics of the waveform, especially the smaller-amplitude oscillations following the first large wave, can be readily varied by introducing disturbances, particularly turbulence, into the flame. This implies that the form is dictated by reflections and/or interference from density gradients within the flame, though no analysis was attempted. Perhaps in a more carefully controlled experiment probing those gradients, useful information could be obtained from the waveform.

It was originally hoped that the waveform might provide information on the bulk energy transfer rates within the flame. Now, a sound wave having a frequency of the order of the inverse of some relaxation time (e.g., a vibrational energy transfer rate) within the system will undergo attenuation and phase shifts due to that relaxation process. Vibrational relaxation times at 1 atm are of the order of the laser pulse duration. The laser pulse thus is expected to produce a spectrum of sound frequencies, and it was hoped that a Fourier analysis of the opto-acoustic waveform

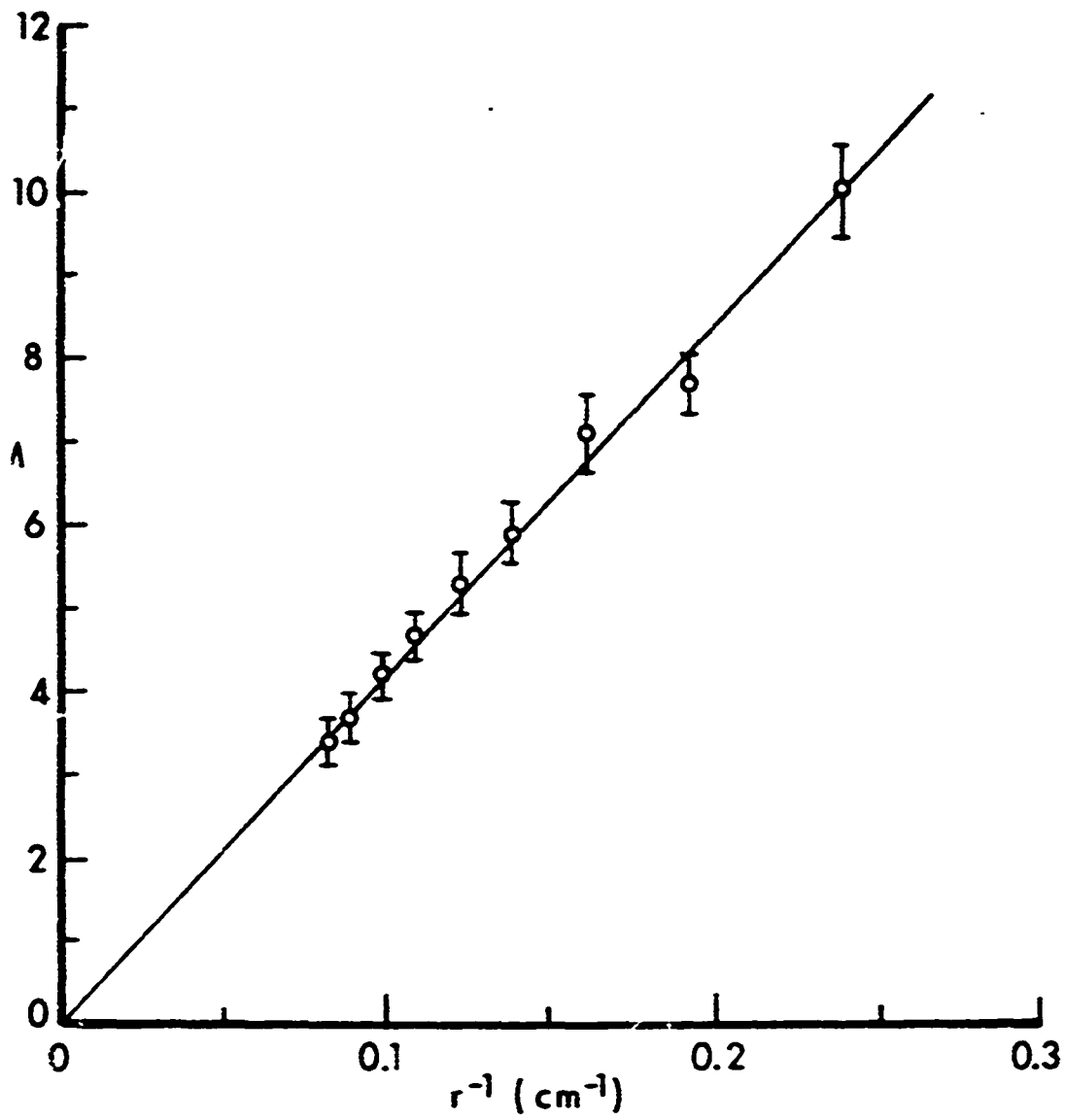


Figure 5. Dependence of pressure wave amplitude on flame-to-microphone distance r .

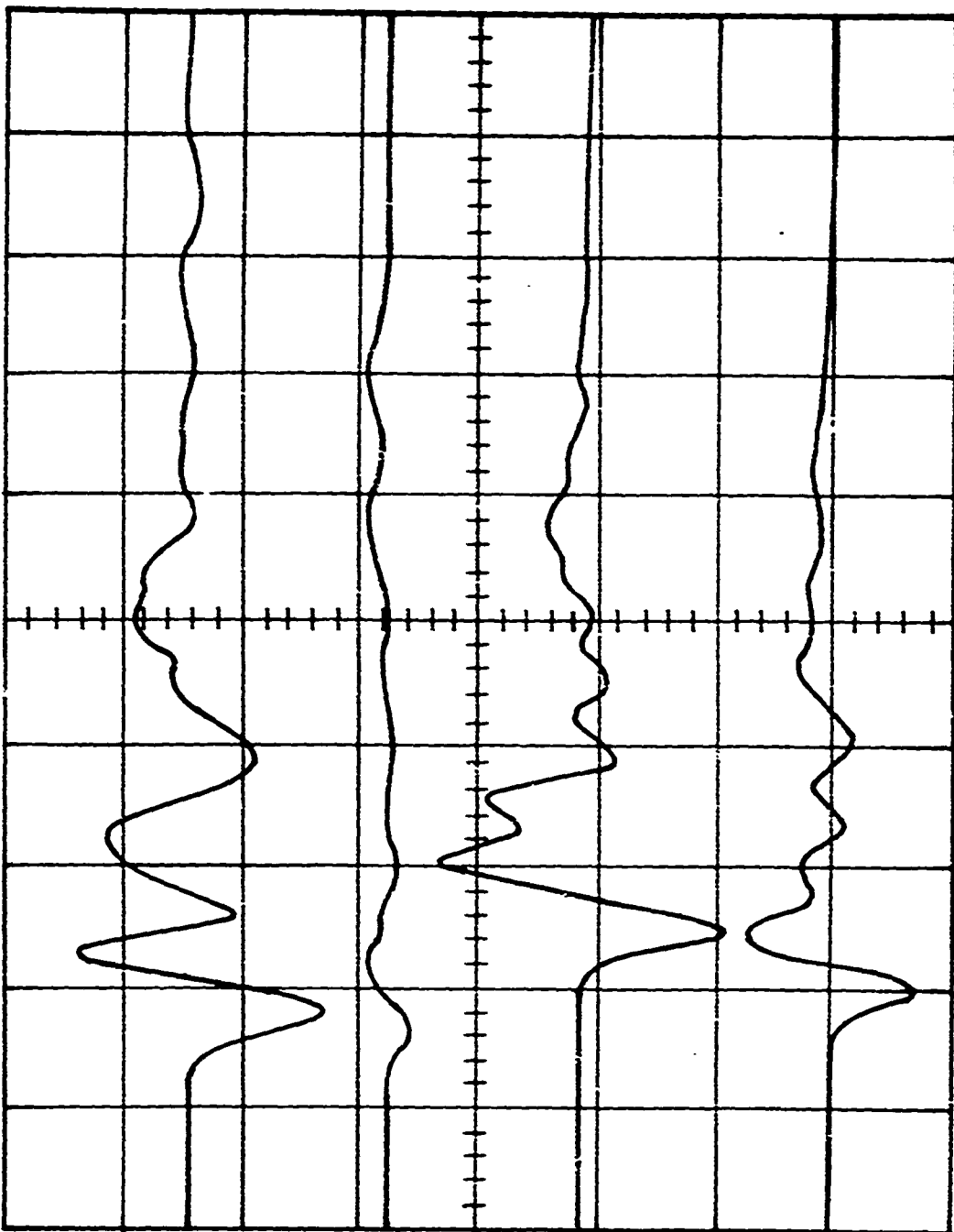


Figure 6. Oscilloscope traces of opto-acoustic signal waveform, for 4 different geometrical arrangements. Each results for a single laser pulse. Horizontal axis: 20 nsec per major division.

might yield information on these relaxation times within the flame. This approach was not successful, due to the dominance of the density gradient effects and the bandwidth (140 kHz) of our fastest microphone. "Air" mixtures of N₂/O₂, Ar/O₂, and CO₂/O₂ were tried in this series of experiments, but no differences could be discerned. With a faster microphone it remains possible that this will be a useful application of this technique.

Even though the vibrational relaxation could not be directly observed in this manner, it is safe to conclude that the energy is transferred through the internal levels of the flame gases. N₂, which constitutes some 60% of the total gas flow, has long been known to have a very high quench rate for electronically excited alkalis, especially Na.

In a short series of experiments, three different microphones of varying diameter were used in order to ascertain whether the frequency response (directly related to the microphone diameter) affected the relative signal size when other parameters were varied. Figure 7 shows a plot of microphone signal vs. beam diameter (the significance is related to the quenching/saturation studies discussed below). It can be seen that the microphone diameter does not affect relative response for these experiments.

III. APPLICATIONS AS A PROBE

A. Concentration Measurements

It has already been demonstrated that the formation of the opto-acoustic pulses introduces a negligible perturbation into the flame gases, insofar as either the chemical kinetics or gas dynamics is concerned. Here we consider the use of the technique as a sensitive probe of selective absorption of laser radiation, i.e., as an alternative or complement to laser excited fluorescence.

Our simple picture of E-V-T transfer and local translational heating suggests that the pressure wave amplitude should be proportional to the laser power and to the concentration of the Na atoms. Figures 8 and 9 show the dependence of the microphone signal on these two parameters. The power dependence is measured at a sufficiently low power density so as to be in the linear absorption region, that is, we do not approach optical saturation in Figure 8. In Figure 9, the microphone signal is plotted against the concentration of the NaI solution aspirated into the flame. The nonlinear curve-of-growth form of the plot reflects the effect of increasing optical thickness. The results shown here demonstrate that we may scale our observed signals to lower Na concentrations and, with due regard to optical saturation, to higher laser power.

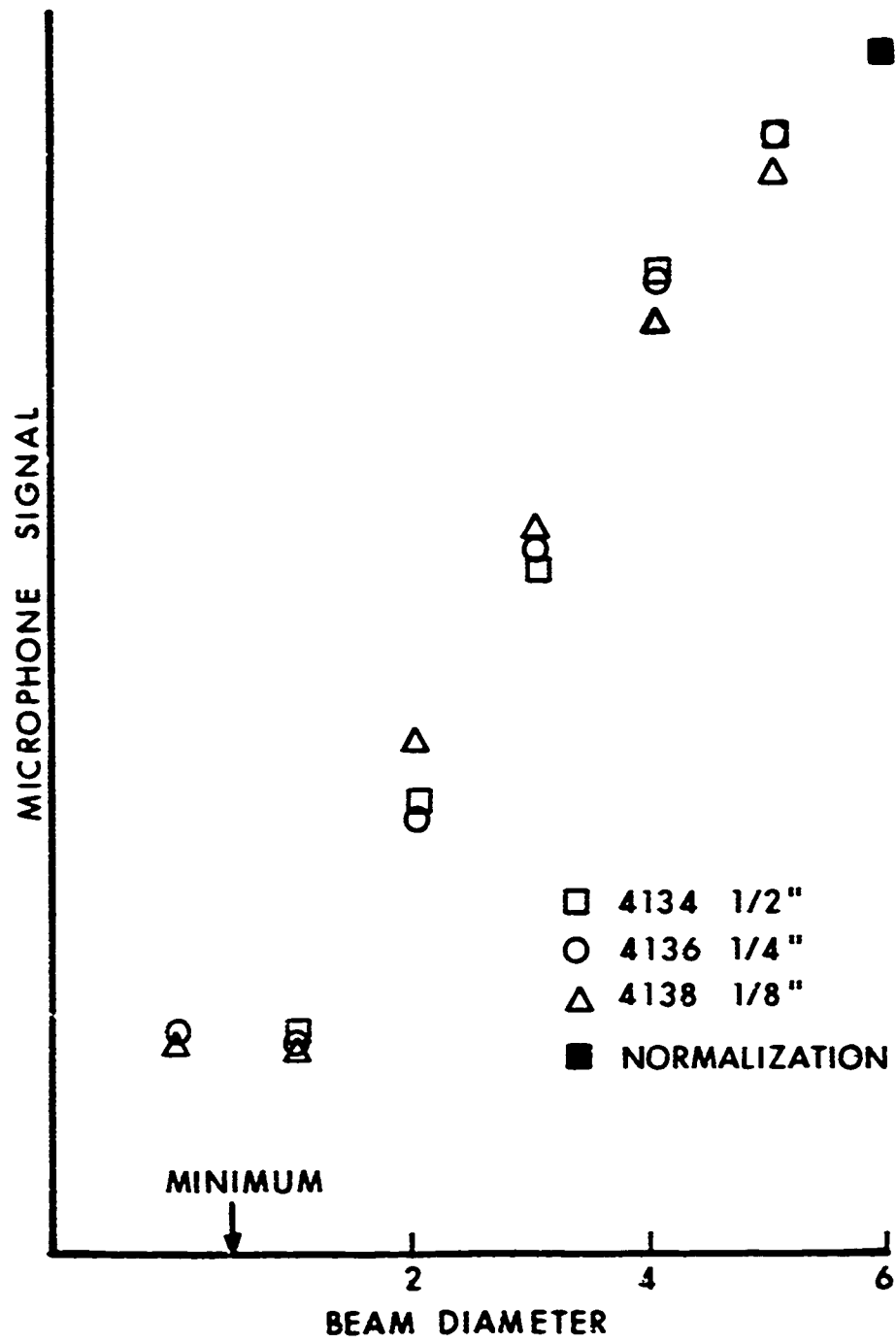


Figure 7. Microphone signal as a function of beam diameter (related to the optical saturation studies) showing that microphones of three different diameters yield the same relative response.

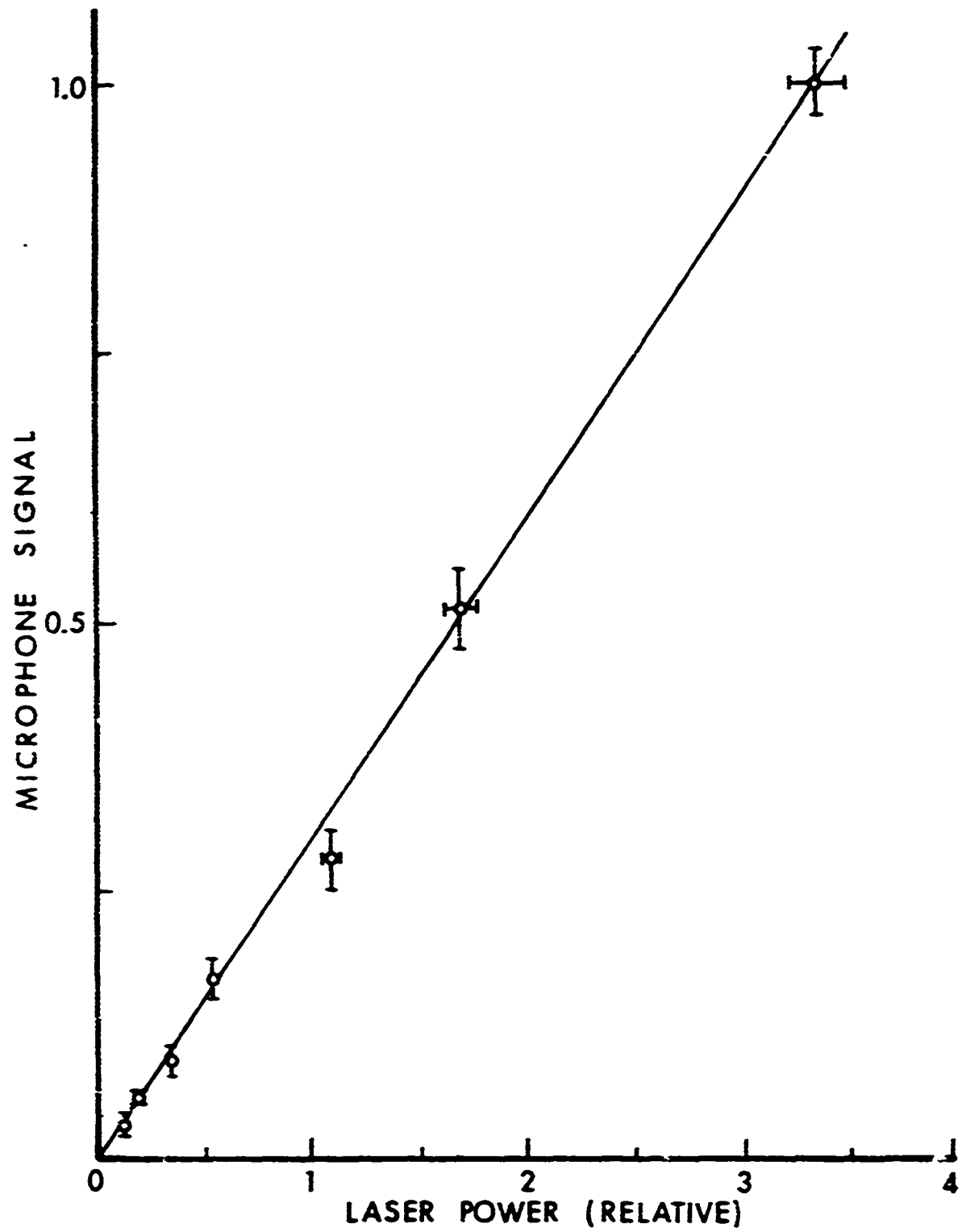


Figure 8. Dependence of the microphone signal on laser power, at power densities much lower than saturation values.

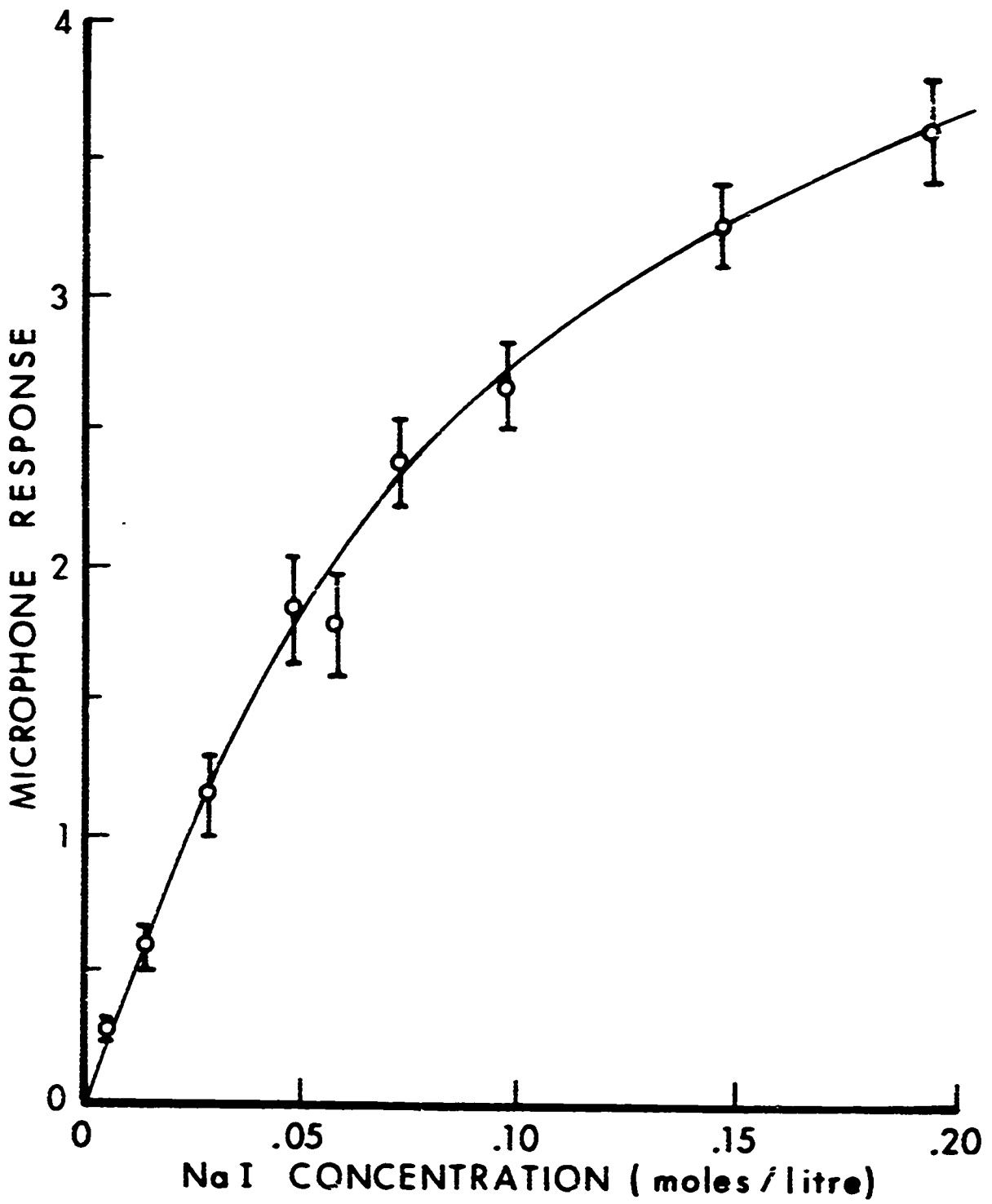


Figure 9. Dependence of the microphone signal on NaI concentration; presumably the Na concentration in the flame follows the solute concentration.

From these guidelines, we may project from our observed signal sizes and background noise a detectability limit for Na. We estimate that with a time constant of about 1 sec (corresponding to averaging over 30 laser pulses), a signal-to-noise ratio of about 2:1 should be obtainable for Na densities of the order of 10^7 atoms per cm^3 in our 1 atm flame. Although this is not as low a limit as one can obtain using laser-excited fluorescence for this species, opto-acoustic pulses nonetheless do constitute a sensitive detection technique. It should be emphasized that we have undertaken no effort to shield the microphone from extraneous sources (pumps, etc.) of background noise; perhaps with two microphones and differencing techniques the noise could be considerably reduced.

Although at higher total number densities, the quantum yield of fluorescence is reduced due to the higher frequency of collisions, the opto-acoustic signal should remain essentially constant. Consequently, this may be the method of choice for some experiments carried out at high pressure.

In addition, there may be some systems which exhibit selective absorption of laser radiation but which do not readily fluoresce. For example, a triatomic or larger molecule may undergo rapid intersystem crossing into a state of different multiplicity from the ground state before fluorescing. Collisions then would remove the energy of excitation before any long-lived phosphorescence would occur. However, the collisional transfer would still result in the formation of a pressure wave upon conversion into translational energy. Another molecular situation might be a case in which the excited molecular state predissociates; pressure waves would be produced upon resonant tuning provided that the absorption lines are still relatively sharp and not all of the absorbed photon energy goes into breaking the chemical bond.

B. Temperature Measurements: Speed of Sound

The pulsed sound wave formation offers the ability to measure the speed of sound, u_s , within the flame; u_s can then be related to the translational temperature, providing an important means of characterizing the flame.

To measure the speed of sound *in situ*, the laser beam is fired into the flame at a particular point, as illustrated in Figure 10. The scope (or boxcar) is triggered at the time of the laser pulse, so that the arrival time of the pressure wave at the microphone can be accurately measured. The laser beam is then moved within the flame (a 1 cm shift is indicated in the figure). The difference in arrival times for the different points, together with the distance between them, furnishes the speed of sound within the flame. (Although the measurements carried out were made by physically moving the beam, a better method would be to split the beam into two or three components and obtain the information from one laser pulse, thus adding time resolution.)

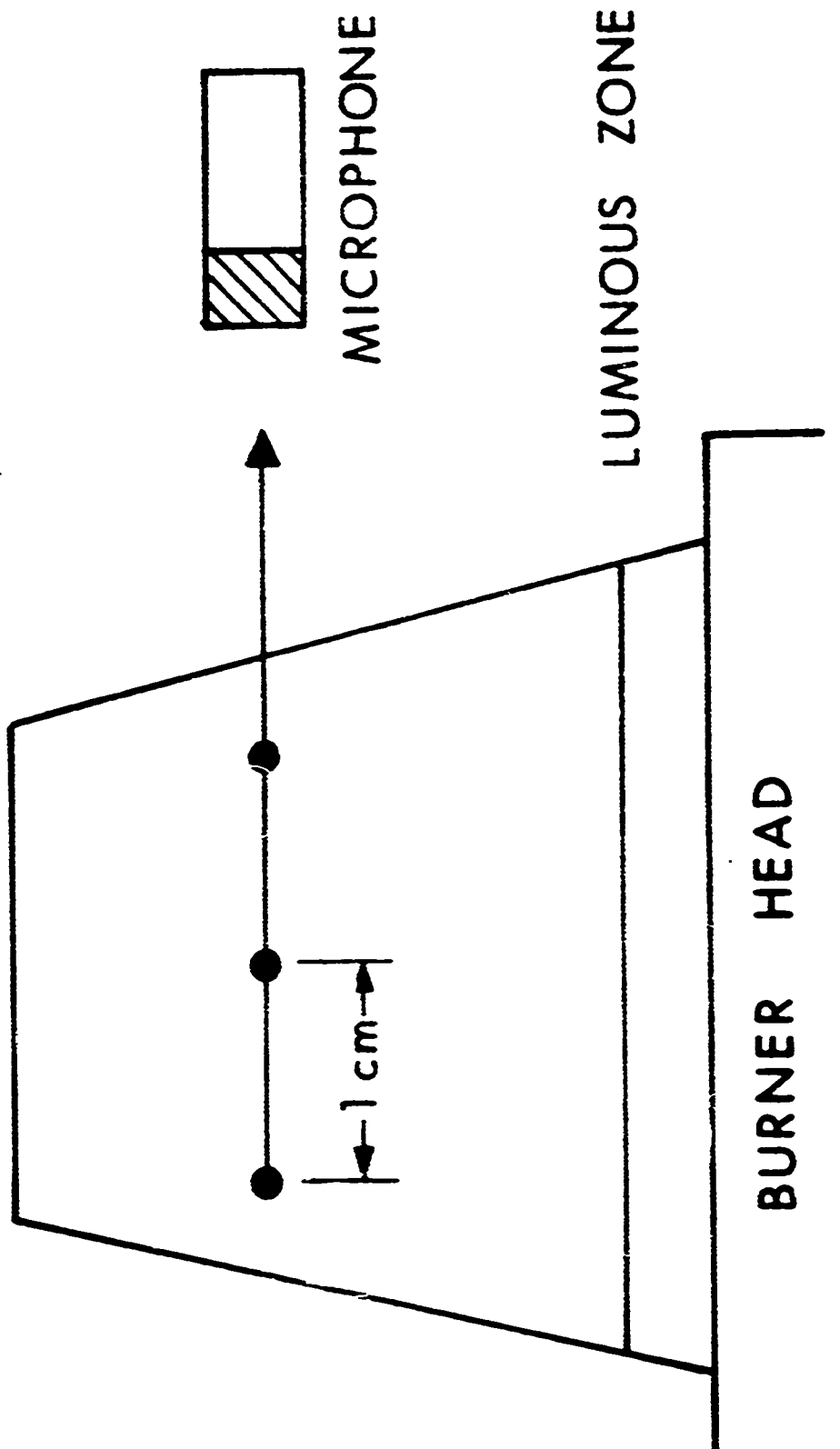


Figure 10. Schematic illustration of the measurement of the speed of sound. On three different laser pulses, the laser beam is fired into the flame at three different positions, and the arrival time of the pressure pulse at the microphone is measured.

The measurements were made at three different heights well into the region of partially burned gases. The results were all the same, $(9.7 \pm 0.5) \times 10^4$ cm sec⁻¹, within experimental error. The uncertainty could be reduced by a more careful measurement of distances than was done for this demonstration experiment.

For a gas of average molecular weight \bar{M} and average heat capacity ratio $\bar{\gamma}$, the speed of sound u_s is related to the translational temperature by

$$u_s = [\bar{\gamma}RT/\bar{M}]^{1/2}. \quad (1)$$

From the stoichiometric composition of the initial flame gases, and reasonable assumptions on the degree of combustion, average values were calculated for \bar{M} (molecular weight) and $\bar{\gamma}$ (heat capacity ratio). Since most of the flame gas is made up of N₂, this is not a critical pair of numbers. These values are then used to calculate the temperature using Eq (1). The result is $2280 \pm 230^\circ\text{K}$, which may be compared to the adiabatic flame temperature for this flame⁶ of 2545°K .

The translational temperature is a most important flame characteristic, from the standpoint of both the gas dynamics and the chemical kinetics. The opto-acoustic pulse method offers the possibility of measuring the closely related speed of sound on a basis of high spatial and temporal resolution. No perturbation such as a thermocouple need be introduced into the flame, and extremely high temperatures (which are hostile to non-optical probes) appear to pose no fundamental difficulties. Such speed of sound measurements could well form the unique contribution of this method as a combustion diagnostic tool.

Of course, by carrying out an excitation scan over a series of molecular absorption lines or bands, using opto-acoustic pulses or fluorescence for detection, one can measure population distributions corresponding to the temperatures of internal degrees of freedom as well.

In addition, the optoacoustic pulse method furnishes the ability to generate pulsed sound waves locally within the flame, so as to study their propagation through the flame gases, the interface with the ambient environment, and the surrounding air. This may be of utility in studies of noise pollution caused by combustion.

⁶A. G. Caydon and H. G. Wolfhard, Flames: Their Structure, Radiation and Temperature, 3rd Ed., Chapman and Hall, London, 1970.

IV. QUENCH RATE MEASUREMENTS

Descriptive Equations:

Under conditions of high laser intensity, one may create an appreciable population in the electronically excited state. This will be the case when the rate, per atom, for absorption of laser light becomes comparable to the rate at which the atoms exit the upper state. Then, the number of excited atoms is no longer linear in the laser intensity.

With a focused laser beam, it is easy to obtain energy densities approaching saturation of the optical transition in Na, even for the high quenching rates found in atmospheric-pressure flames. Daily⁷ has suggested operation in this regime to obviate the need for quenching rates to analyze laser-excited fluorescence data, and recently Baronavski and McDonald⁸ have used fluorescence measurements and a series expansion of the fluorescent signal equation to measure the quenching of C₂ in a flame. Using the optoacoustic pulses, we have measured the total quenching rate for Na in the acetylene-air flame.

We consider a two-level system (see Figure 11) and write a steady-state equation for the excited state number density N_e.

$$\frac{dN_e}{dt} = 0 = BIN_g - (BI + Q + A)N_e. \quad (2)$$

The assumption of a steady state is valid since the time scales involved for the absorption and quenching processes are significantly shorter than the laser pulse duration. Here, B and A are the Einstein coefficients for absorption and spontaneous emission, respectively; the term BIN_e accounts for stimulated emission. I is the laser spectral power density measured in (erg/sec) per cm² per unit frequency interval. Q is the total quench rate, per sec, for the upper level.

Since the total Na number density is a constant N₀. i.e.

$$N_e + N_g = N_0.$$

⁷J. H. Daily, "Saturation Effects in Laser-Induced Fluorescence Spectroscopy", *Appl. Opt.* 16, 568-571 (1977).

⁸A. P. Baronavski and J. R. McDonald, "Measurement of C₂ Concentrations in an Oxygen-acetylene Flame: An Application of Saturation Spectroscopy", *J. Chem. Phys.* 66, 3300-3301 (1977); A. P. Baronavski and J. R. McDonald, "Application of Saturation Spectroscopy to the Measurement of C₂, S_{1,u} Concentrations in Oxy-acetylene Flames", *Appl. Opt.* 16, 1897-1901 (1977).

QUENCHING IN LASER-EXCITED FLUORESCENCE

- 1) Low laser power
(2-level model)

$$F = \frac{ABIN_0}{A+Q}$$

- 2) High laser power
(2-level model)

$$F = \frac{ABIN_0}{A+Q+B}$$

- 3) Multi-level model

must incorporate relaxation rates R , R depending on levels monitored

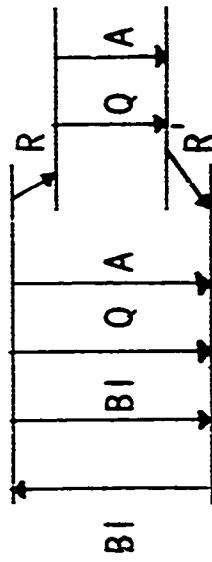
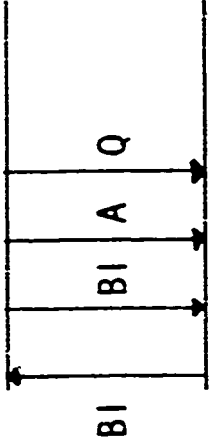
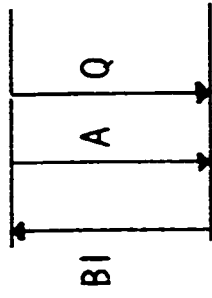


Figure 11. Schematic illustration of a system near optical saturation. Two level models are illustrated in (1) and (2); it is these which are pertinent to the treatment in the text. The multi-level model (3) requires the incorporation of relaxation rate parameters.

Eq. (2) may be solved for the steady-state value of N_e

$$(N_e)_{s.s.} = \frac{BIN_0}{Q+A+2BI} . \quad (3)$$

Now the opto-acoustic pulse signal M is proportional to $(N_e)_{s.s.}$:

$$M = c(N_e)_{s.s.} ,$$

where the constant represents the efficiency of conversion of electronic to translational energy, the microphone and amplifier characteristics and geometrical considerations. Substituting into Eq. (2), one has for the inverse of the microphone signal

$$M^{-1} = c' [2 + \left(\frac{Q+A}{B}\right)\frac{1}{I}] . \quad (4)$$

Thus a plot of M^{-1} (in arbitrary units) vs. I^{-1} (in absolute units) should yield a straight line with a slope to intercept ratio of

$$\frac{Q+A}{2B} = \frac{Q/A+1}{2B/A} . \quad (5)$$

The relationship between B and A is known from thermodynamic considerations:

$$B = \frac{\lambda^5}{2hc} A , \quad (6)$$

so that the experimental result serves to determine Q/A . But if A has been separately measured, then an absolute value of Q may be extracted.

It may be parenthetically noted that these simple equations pertain to a two-level model only. Sodium itself has three levels participating in this process, the $^2S_{1/2}$, $^2P_{1/2}$, and $^2P_{3/2}$. Taking into account the transfer between the upper doublet components, which requires a separate fluorescence scan of the D-line emission, one may still obtain an analysis of the data. This refinement for Na is discussed in Ref. 2. For a yet more complicated system such as a molecule with a series of rotational levels among which energy transfer may occur, the equations

become considerably more complex and require much more independent information on the energy transfer cross sections. Theoretical considerations of such a system are currently being pursued at the Ballistic Research Laboratory.⁹

We nonetheless proceed with an analysis of the present data in terms of a two-level model, in order to assess its utility. An examination of Eq. (4) shows that if the laser intensity is varied over a range far lower than saturation, the effective intercept will be zero. This is illustrated for an unfocussed laser beam in Figure 12, where the spectral power density is here given in $\text{erg cm}^{-2} \text{ sec}^{-1} \text{ Hz}^{-1}$. The experiment was repeated after focussing the laser to a beam diameter one third the size, resulting in power densities an order of magnitude larger. These results are plotted in Figure 13. The low power levels of Figure 12 do not permit the distinction of a non-zero intercept, beyond experimental error bars, although the finite intercept is readily apparent in Figure 13.

Figure 14, shows a plot of the data for one run, in the form of Eq. (4). The error bars represent estimates of the readability of the boxcar signals; the line is an unweighted least squares fit to the data. In this instance we obtain $Q/A = 410 \pm 40$. Using the value $A = 6.3 \times 10^7 \text{ sec}^{-1}$, this results in a $Q = (2.6 \pm 0.5) \times 10^{10} \text{ sec}^{-1}$.

This is too large, by comparison with calculated values using previously determined cross sections for the quenching collisions¹⁰. Part of the problem is due to the Gaussian nature of the laser beam spatial profile,¹¹ and our choice of intensity/range and Na density. Reference 2 contains more realistic results combining the opto-acoustic pulse measurements with fluorescence results. Nonetheless, these results clearly demonstrate that the opto-acoustic pulse method forms a useful detection technique.

V. 4P LEVEL PUMPING

Excitation to the 4P level is provided by frequency doubling the laser to the resonance wavelength of 3303Å. Although the oscillator strength of this transition is low, we can operate at high enough Na density to observe measurable excitation, as confirmed by fluorescence

⁹A. H. Gelb, A. J. Kotlar and D. R. Crosley, "Response of a Molecular System to Optical Excitation Under Saturation Conditions", to be published.

¹⁰P. Hoorniers and C. Th. J. Alkemade, "Quenching of Excited Alkalies Atoms and Related Effects in Flames. Part II. Measurements and Discussion", *J. Quant. Spectr. Rad. Transf.* 6, 847-874 (1965).

¹¹J. W. Daily, "Saturation of Fluorescence in Flames with a Gaussian Beam", *Appl. Opt.* 17, 225-229 (1978).

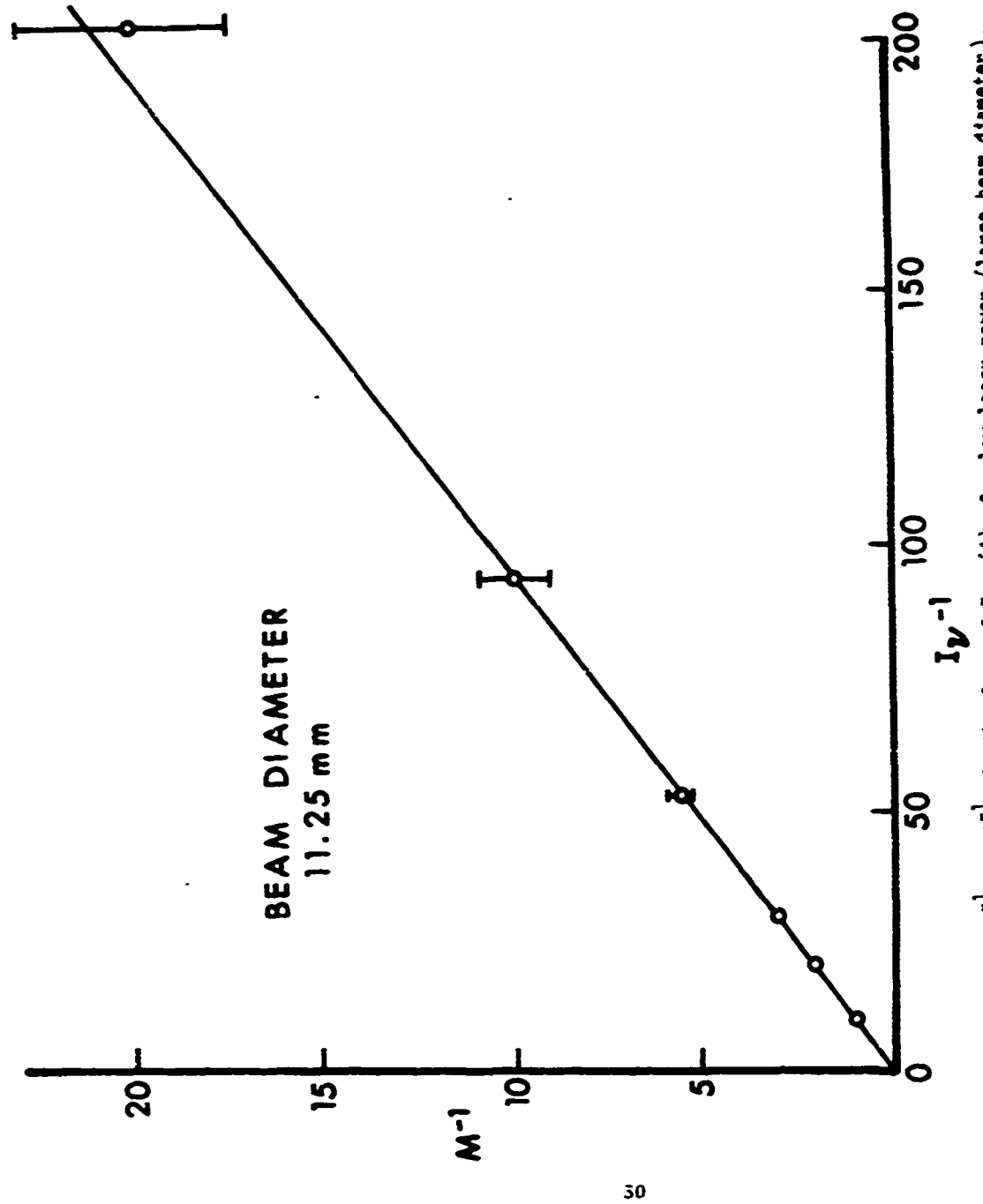


Figure 12. Plot of M^{-1} vs. I^{-1} , in the form of Eq. (4), for low laser power (large beam diameter).

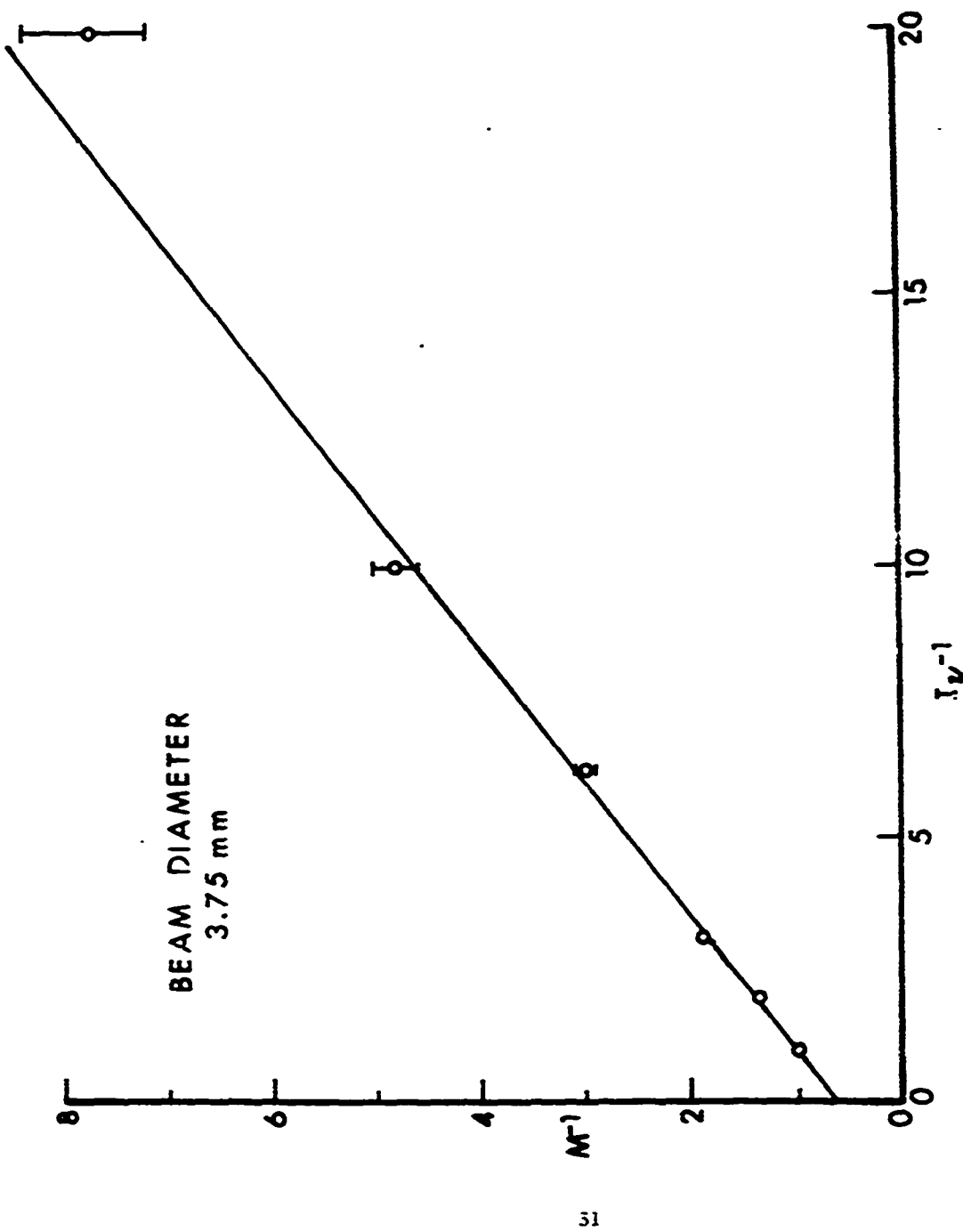


Figure 13. Plot of M^{-1} vs. I_V^{-1} , in the form of Eq. (4), for high laser power (focussed beam).

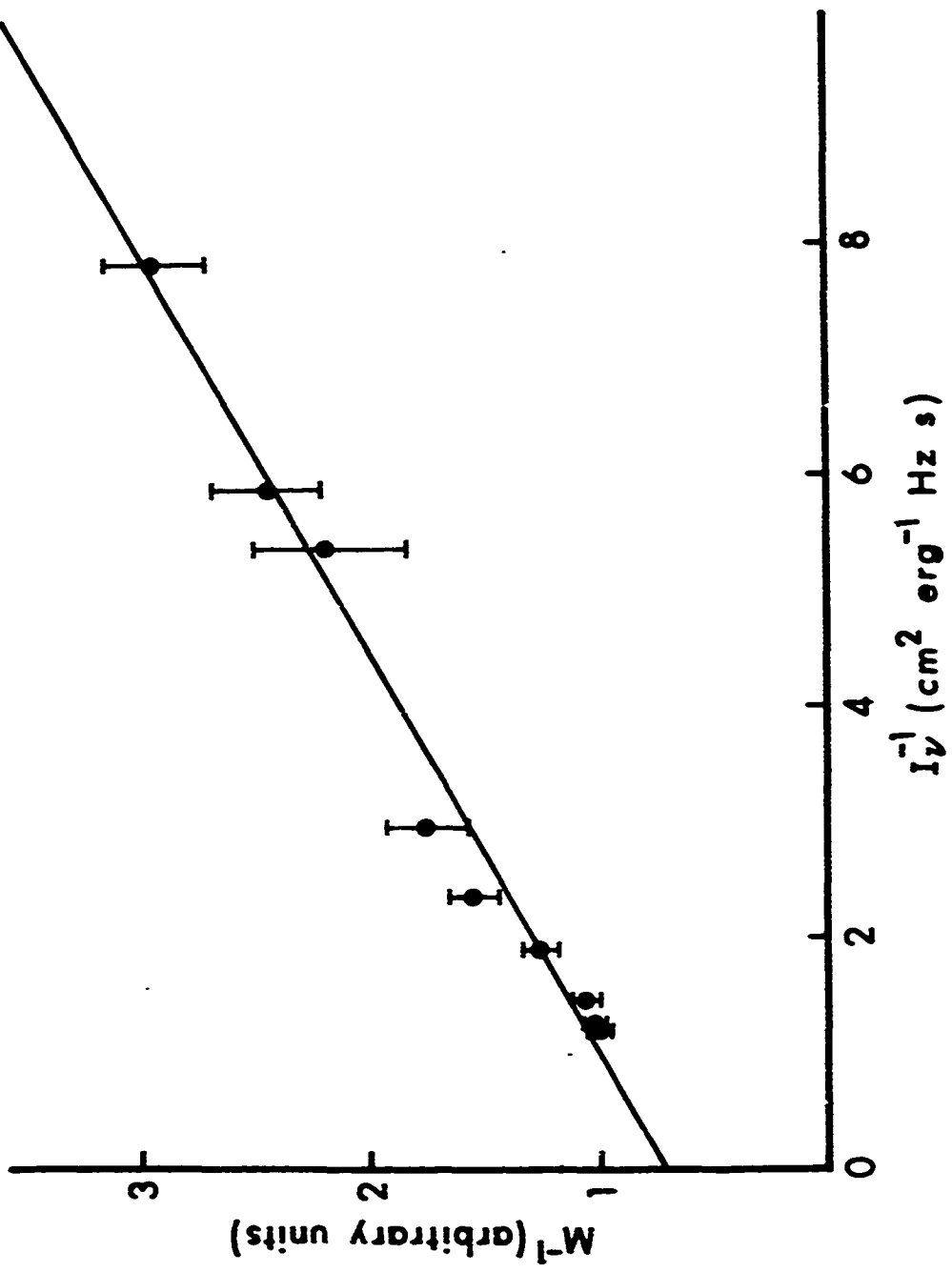


Figure 14. Inverse of the pressure-wave amplitude versus inverse of the spectral-power density. Error bars represent estimates of the readability of the boxcar output. The line is an unweighted least-squares fit.

from the 4P level itself, as well as from other levels populated by collision (see below). Using the amount of energy absorbed, we may estimate the size of the expected opto-acoustic pulse signal in a manner similar to that outlined above for the 3P level. The anticipated value is 18 mTorr at the microphone, but no signal is observed above the background noise level of 0.2 mTorr.

We find the absence of an opto-acoustic signal from this higher-lying level quite surprising. One possibility is that there exists a markedly different rate either for direct quenching of the 4P level itself, or for the rate of subsequent V to T transfer in the flame gases. If the energy were to be trapped in internal modes, it might not form as sharply defined an initially heated region and thus might yield a sound wave much reduced in amplitude. Another possibility is that the 4P level is removed rapidly by chemical reaction, so that little of the electronic energy is converted into translational energy. Although this latter phenomenon has been seen to exist in flames for the 3P level,¹² it would have to be much faster than observed there in order to compete with collisional quenching in our system.

Further information about relative quench and energy transfer rates is obtained from observations using two-photon excitation.² There, the laser was tuned to the wavelength corresponding to half the energy difference between the 3S state and the 3D, 5S or 4D state. Observations were made of emission from all four high-lying states when the laser is tuned to excite each one of them, in turn. Ratios of the populations of these levels were obtained from ratios of the fluorescence intensities and inserted into steady-state rate equations describing the collisional energy transfer. By invoking detailed balancing to relate upward and downward transfer rates between pairs of states, a determination was made of all ten transfer rates among the four levels as well as the total quenching rates out of each state, normalized to the value of one of them.

It may be seen from the results of Reference 2 that the 4P level does indeed possess a collisional loss rate (at least in this flame) which is considerably smaller than that of the other nearby levels. On the other hand, the absolute quench rate still remains high, faster than one quenching collision per nsec. This value is obtained from our measurements on the 3P level together with quenching cross sections for N₂ obtained from low pressure experiments on both the 3P¹⁰ and 4P¹³ levels. Consequently, there would appear to be no energy bottleneck attributable to at least the E to V aspect of the energy transfer.

¹²C. H. Muller III, K. Schofield and M. Steinberg, "Near Saturation Laser Induced Chemical Reactions of Na ($3^2P_{3/2, 1/2}$) in H₂/O₂/N₂ Flames", Chem. Phys. Letters 57, 364-368 (1978).

¹³T. F. Gallagher, W. E. Cooke and S. A. Edelstein, "Collisional Deactivation of the 5s and 4p States of Na by N₂", Phys. Rev. A17, 125-131 (1978).

If the quenching of the 4P level returned the Na predominantly to the ground (3S) state, then about twice as much energy would be transferred to the vibrational levels of the flame gases as occurs in a 3P to 3S quenching collision. This would populate a different set of vibrational levels in the flame gases, and conceivably one could have a different mode of V to T transfer and slower formation of the pressure wave. However, the results of Reference 2 argue against this possibility as well. It is seen from those state-to-state transfer rates that half of the transfer out of the 4P leaves the Na atom in the 5S, 4D or 3D level (mostly the 3D). Much of the remainder is likely to terminate on the 3P, as fluorescence is observed originating from that level as well. (In fact, the results of Reference 2 show altogether convincing evidence of step-wise relaxation in the flame, as opposed to a direct return to the ground state. There is a smooth decrease of energy transfer probability with energy defect. This fact has important implications for treating, in a microscopic way, the occurrence of non-equilibrium populations, especially of reactive species, within high temperature systems.) As a result, it appears that a similar range of vibrational levels in the flame gases participate in the E \rightarrow V \rightarrow T transfer out of the 4P level and the 3P level.

The small value of Q(4P) from Reference 2, which necessarily includes reactive collisions as well, and the size of k(4p \rightarrow 3d) suggest that reaction of the 4P level does not occur rapidly. We thus do not understand why the 4P level excitation does not produce opto-acoustic pulses. Perhaps the answer lies in more detailed understanding of the dynamical formation of the pressure wave.

VI. CONCLUSIONS

We have described a new type of opto-acoustic effect -- the production of pulsed sound waves in an atmospheric pressure flame following deposition of a laser pulse into electronic energy levels. The experiments on Na demonstrate that good signal to noise ratios can be obtained at sub-ppb levels of the seeded atoms, using a commercially available laser of modest power. (We add that opto-acoustic signals have also been observed by pumping Na in the C₂H₂-air flame using a dye laser pumped by a N₂ laser; a more quantitative study may reveal further details concerning the formation of the pressure wave, since the dye laser pulse is in this case only several nsec long as opposed to 1 μ sec for the flashlamp-pumped laser.)

The opto-acoustic pulse signal thus forms a sensitive detector of selective absorption of laser radiation. There appears to be no fundamental reason why the technique should not be applicable to other species, including in particular molecular absorption systems. We remain mystified, however, by the lack of opto-acoustic signal from the Na 4P excitation, which suggests that the situation is not entirely straightforward and should be approached on a case-by-case basis. Nonetheless, we feel

that there is promise for the technique simply as a detection mode, particularly for species which absorb laser radiation but do not fluoresce readily (either due to high pressure or the rapid crossing into a non-fluorescing state).

The form of the pressure pulse produced, if it yields to analysis, holds information on density gradients within the flame and perhaps on relaxation phenomena within the flame gases. For the investigations of quenching in Na under conditions approaching optical saturation, detection via opto-acoustic pulses provides a measure of the excited state number density under conditions in which fluorescence detection is hampered by self-absorption problems. It may thus be a useful complement to fluorescence in experiments designed to probe behavior near saturation over a wide range of Na density.

Finally, and perhaps most important, the method affords the ability to produce locally within the flame a pulsed sound wave. This has provided rapid and spatially resolved measurements of the speed of sound within the combusting system, and could form a useful tool to generate sound waves for an investigation of the noise produced by flames.

REFERENCES

1. A. C. Eckbreth, P. A. Bonczyk and J. F. Verdieck, "Review of Laser Raman and Fluorescence Techniques for Practical Combustion Diagnostics", United Technologies Research Center Report R77-952665-6, Hartford, CT, February 1977.
2. J. E. Alien, Jr., W. R. Anderson, D. R. Crosley and T. D. Fansler, "Energy Transfer and Quenching Rates of Laser-Pumped Electronically Excited Alkalies in Flames", Seventeenth Symposium (International) on Combustion, Leeds, England, August 1978.
3. D. Hartley, M. Lapp and D. Hardesty, "Physics in Combustion Research", Physics Today, December 1975, 36-47.
4. R. B. Green, R. A. Keller, P. K. Schenck, J. C. Travis and C. G. Luther, "Opto-Galvanic Detection of Species in Flames", J. Amer. Chem. Soc. 98, 8517-8518 (1976).
5. H. Y. Pao (ed.), Optoacoustic Spectroscopy and Detection, Academic Press, New York, 1977.
6. A. G. Gaydon and H. G. Wolfhard, Flames: Their Structure, Radiation and Temperature, 3rd Ed., Chapman and Hall, London, 1970.
7. J. W. Daily, "Saturation Effects in Laser-Induced Fluorescence Spectroscopy", Appl. Opt. 16, 568-571 (1977).
8. A. P. Baronavski and J. R. McDonald, "Measurement of C₂ Concentrations in an Oxygen-acetylene Flame: An Application of Saturation Spectroscopy", J. Chem. Phys. 66, 5300-5301 (1977); A. P. Baronavski and J. R. McDonald, "Application of Saturation Spectroscopy to the Measurement of C₂, S_{3/2} Concentrations in Oxy-acetylene Flames", Appl. Opt. 16, 1897-1901 (1977).
9. A. H. Gelb, A. J. Kotiar and D. R. Crosley, "Response of a Molecular System to Optical Excitation Under Saturation Conditions", to be published.
10. P. Hoomayers and C. Th. J. Alkemade, "Quenching of Excited Alkalies Atoms and Related Effects in Flames. Part II. Measurement and Discussion", J. Quant. Spectr. Rad. Transf. 6, 847-874 (1966).
11. J. W. Daily, "Saturation of Fluorescence in Flames with a Gaussian Beam", Appl. Opt. 17, 225-229 (1978).
12. C. H. Muller III, K. Schofield and M. Steinberg, "Near Saturation Laser Induced Chemical Reactions of Na (3²P_{3/2,1/2}) in H₂/O₂/N₂ Flames", Chem. Phys. Letters 57, 364-368 (1978).

REFERENCES (continued)

13. T. F. Gallagher, W. E. Cooke and S. A. Edelstein, "Collisional Deactivation of the 5s and 4p States of Na by N₂", Phys. Rev. A17, 125-131 (1978).

DISTRIBUTION LIST

<u>No. of Copies</u>	<u>Organization</u>	<u>No. of Copies</u>	<u>Organization</u>
12	Commander Defense Technical Infor ATTN: DDC-DDA Cameron Station Alexandria, VA 22314	1	Commander US Army Armament Materiel Readiness Command ATTN: DRSAR-LEP-L, Tech Lib Rock Island, IL 61299
1	Director Defense Advanced Research Projects Agency ATTN: LTC. C. Buck 1400 Wilson Boulevard Arlington, VA 22209	1	Director US Army ARRADCOM Benet Weapons Laboratory ATTN: DRDAR-LCB-TL Watervliet, NY 12189
2	Director Institute for Defense Analyses ATTN: H. Wolfhard R.T. Oliver 400 Army-Navy Drive Arlington, VA 22202	1	Commander US Army Watervliet Arsenal ATTN: Code SARWV-RD, R. Thierry Watervliet, NY 12189
1	Commander US Army Materiel Development and Readiness Command ATTN: DRCDMD-ST 5001 Eisenhower Avenue Alexandria, VA 22353	1	Commander US Army Aviation Research and Development Command ATTN: PRSAV-E F.O. Box 209 St. Louis, MO 63166
2	Commander US Army Armament Research and Development Command ATTN: DRDAR-TSS Dover, NJ 07801	1	Director US Army Air Mobility Research and Development Laboratory Ames Research Center Moffett Field, CA 94035
4	Commander US Army Armament Research and Development Command ATTN: DRDAR-LCA, J. Lannon DRDAR-LC, J.P. Picard DRDAR-LCE, R.F. Walker DRDAR-SCA, L. Stiefel Dover, NJ 07801	1	Commander US Army Communications Research and Development Command ATTN: DRDCO-PPA-SA Ft. Monmouth, NJ 07703
		1	Commander US Army Electronics Research and Development Command Technical Support Activity ATTN: DELSD-L Ft. Monmouth, NJ 07703

DISTRIBUTION LIST

<u>No. of Copies</u>	<u>Organization</u>	<u>No. of Copies</u>	<u>Organization</u>
1 Commander	US Army Missile Command ATTN: DRSMI-R Redstone Arsenal, AL 35809	1 Office of Naval Research	ATTN: Code 473 800 N. Quincy Street Arlington, VA 22217
1 Commander	US Army Missile Command ATTN: DRSMI-YDL Redstone Arsenal, AL 35809	1 Commander	Naval Sea Systems Command ATTN: J.W. Murrin (SEA-62R2) National Center Bldg 2, Room 6E08 Washington, DC 20362
1 Commander	US Army Natick Research and Development Command ATTN: DRXRE, D. Sieling Natick, MA 01762	1 Commander	Naval Surface Weapons Center ATTN: Library Br, DX-21 Dahlgren, VA 22448
1 Commander	US Army Tank Automotive Research and Development Command ATTN: DRDTA-UL Warren, MI 48090	2 Commander	Naval Surface Weapons Center ATTN: S.J. Jacobs/Code 240 Code 730 Silver Springs, MD 20910
1 Commander	US Army White Sands Missile Range ATTN: STEWS-VT WSMR, NM 88002	1 Commander	Naval Underwater Systems Center Energy Conversion Department ATTN: R.S. Lasar/Code 5B331 Newport, RI 02840
1 Commander	US Army Materials & Mechanics Research Center ATTN: DRXMR-ATL Watertown, MA 02172	2 Commander	Naval Weapons Center ATTN: R. Derr C. Thelen China Lake, CA 93555
1 Commander	US Army Research Office ATTN: Tech Lib Research Triangle Park, NC 27706	1 Commander	Naval Research Laboratory ATTN: Ccde 6180 Washington, DC 20375
1 Director	US Army TRADOC Systems Analysis Activity ATTN: ATAA-SL, Tech Lib White Sands Missile Range, NM 88002	3 Superintendent	Naval Post Graduate School ATTN: Tech Lib D. Netzer A. Fuhs Monterey, CA 93940

DISTRIBUTION LIST

<u>No. of Copies</u>	<u>Organization</u>	<u>No. of Copies</u>	<u>Organization</u>
2	Commander Naval Ordnance Station ATTN: S. Mitchell Tech Lib Indian Head, MD 20640	1	AVCO Corporation AVCO Everett Research Lab Div ATTN: D. Stickler 2385 Revere Beach Parkway Everett, MA 02149
3	AFOSR ATTN: L. Caveny B.T. Wolfson Bolling AFB, DC 20332	1	Bell Laboratories ATTN: A. Tam Murray Hill, NJ 07974
2	AFRPL (DYSC) ATTN: D. George J.N. Levine Edwards AFB, CA 93523	1	Calspan Corporation ATTN: E.B. Fisher P.O. Box 400 Buffalo, NY 14211
4	National Bureau of Standards ATTN: T. Kashiwagi M. Linzer K. Smith Washington, DC 20234	1	Foster Miller Associates, Inc. ATTN: A.J. Erickson 135 Second Avenue Waltham, MA 02154
1	Lockheed Palo Alto Research Lab ATTN: Tech Info Center 3521 Hanover Street Palo Alto, CA 94304	1	General Electric Company Armament Department ATTN: M.J. Bulman Lakeside Avenue Burlington, VT 05402
1	Director NASA Goddard Space Flight Center ATTN: J.E. Allen, Jr. Greenbelt, MD 20770	1	General Electric Company Flight Propulsion Division ATTN: Tech Lib Cincinnati, OH 45215
1	Aerojet Solid Propulsion Co. ATTN: P. Micheli Sacramento, CA 95813	2	Hercules Incorporated Alleghany Ballistic Lab ATTN: R. Miller Tech Lib Cumberland, MD 21501
2	ARO Incorporated ATTN: N. Dougherty W. Williams Arnold AFS, TN 37389	1	IITRI ATTN: M.J. Klein 10 West 35th Street Chicago, IL 60615
1	Atlantic Research Corporation ATTN: M.K. King 5390 Cherokee Avenue Alexandria, VA 22314		

DISTRIBUTION LIST

<u>No. of Copies</u>	<u>Organization</u>	<u>No. of Copies</u>	<u>Organization</u>
1	Olin Corporation Badger Army Ammunition Plant ATTN: J. Ramnarace Baraboo, WI	3	West Virginia University Department of Chemistry ATTN: G. Havrilla Morgantown, WV 26506
5	Olin Corporation New Haven Plant ATTN: R.L. Cook D.W. Fiebler 275 Winchester Avenue New Haven, CT 06504	<u>Aberdeen Proving Ground</u>	
1	Paul Gough Associates, Inc. ATTN: P.S. Gough P.O. Box 1614 Portsmouth, NH 03801	Dir, USAMSA	ATTN: DRXSY-D DRXSY-MP, H. Cohen
1	Phillips Petroleum Company Research and Development Dept ATTN: A.M. Schaffer 124-RBS Bartlesville, OK 74004	Cdr, USATECOM	ATTN: DRSTE-TG-F
10	SRI International ATTN: D. Crosley 333 Ravenswood Avenue Menlo Park, CA 94025	Dir. USACSL, Bldg E3516, EA	ATTN: DRDAR-CLB-PA
6	United Technologies Research Corp. ATTN: A.C. Eckbreth East Hartford, CT 06108		
1	Georgia Institute of Technology ATTN: B.T. Zinn Atlanta, GA 30332		
8	University of Arkansas Department of Physics ATTN: R. Gupta Fayetteville, AK		
5	University of Florida Department of Chemistry ATTN: J. Winefordner Gainesville, FL 32601		